

# Topological charged BPS vortices in Lorentz-violating Maxwell-Higgs electrodynamics

R. Casana, G. Lazar.

<sup>1</sup>*Departamento de Física, Universidade Federal do Maranhão, 65080-805, São Luís, Maranhão, Brazil.*

We have performed a complete study of BPS vortex solutions in the Abelian sector of the standard model extension (SME). Specifically, we have coupled the SME electromagnetism with a Higgs field which is supplemented with a Lorentz-violating CPT-even term. We have verified that Lorentz violation (LV) belonging to the Higgs sector allows to interpolate between some well known models like, Maxwell-Higgs, Chern-Simons-Higgs and Maxwell-Chern-Simons-Higgs. We can also observed that the electrical charged density distribution is nonnull in both CPT-even and CPT-odd models; however, the total electric charge in the CPT-even case is null, whereas in the CPT-odd one it is proportional to the quantized magnetic flux. The following general results can be established in relation to the LV introduced in the Higgs sector: it changes the vortex ansatz and the gauge field boundary conditions. A direct consequence is that the magnetic flux, besides being proportional to the winding number, also depends explicitly on the Lorentz-violation belonging to the Higgs sector.

PACS numbers: 11.10.Lm, 11.27.+d, 12.60.-i, 74.25.Ha

## I. INTRODUCTION

Physics in the context of Lorentz-violating theories have been an important branch for different theoretical and experimental research in recent years. The standard model extension (SME) [1–3] is the general theoretical framework for studying Lorentz violation (LV) effects, and it is build by adding Lorentz-violating terms in all sectors of the minimal standard model. Particularly, the Abelian gauge sector of the SME is the principal focus in searching for LV effects in physical systems [4]–[9].

On the other hand, magnetic flux vortices have gained great interest since Abrikosov's description for Type-II superconductors [10], which arise naturally from the non-relativistic limit of Ginzburg-Landau (GL) theory [11]. In field theory, stable vortex configurations came up with the seminal work by Nielsen and Olesen [12] whose study of the Maxwell-Higgs (MH) model shows that electrically neutral vortex solutions correspond to the ones obtained by Abrikosov. Lately, the existence of electrically charged vortex solutions in Chern-Simons-Higgs (CSH) [13, 14] and Maxwell-Chern-Simons-Higgs (MCSH) [15, 16] models was verified.

The study of topological defects in the context of Lorentz-violating models has been performed in some cases, for example, scalar systems [17], Abelian monopoles [18], tensor fields [19], etc. The research for explicit BPS vortex solutions in the context of SME was recently performed in Refs. [20–24].

The aim of this article is to investigate how LV introduced in Higgs sector affects the structure of topological defects; particularly, we discuss charged BPS vortices in Lorentz-violating MH models. It is easily observed that Higgs's Lorentz-violating term introduces anisotropies in the dispersion relations of the Higgs field. Consequently, these anisotropies provide a Hamiltonian dynamics very similar to GL models describing anisotropic and layered superconductors (e.g. high- $T_c$  superconductors) [25–28]. So, the main motivation for studying topological defects in the context of Lorentz-violating theories comes from

the similitude with the mathematical structure describing the physics of new high- $T_c$  superconductors. These new structures lead to a strong anisotropy of magnetic properties and gives rise to new phenomena, such as formation of two-dimensional vortices and existence of new type of vortex lattices [26, 28].

The manuscript begins by studying the MH model supplemented with a CPT-odd or Carroll-Field-Jackiw (CFJ) term and then with a CPT-even term in gauge sector. In both situations we have introduced a CPT-even and Lorentz-violating term in the Higgs sector. As can be expected, for the first model electrically charged configurations appear due to the CFJ term in the same manner as in MCSH model. For the second model, electric and magnetic sectors are coupled due to parity-odd coefficients presents in the electromagnetic CPT-even and Lorentz-violating term. In the following sections, we analyze in detail both LV scenarios for Abrikosov-Nielsen-Olesen (ANO) vortices.

## II. TOPOLOGICAL CHARGED BPS VORTICES IN A CPT-ODD AND LORENTZ-VIOLATING FRAMEWORK

We consider the Abelian sector of the SME, which corresponds to the MH model supplemented with Lorentz-violating terms [2]. Our first analysis is restricted to the photon sector, including only the CFJ term [4], while the Higgs sector is modified by a CPT-even term,

$$\mathcal{L} = -\frac{1}{4}F_{\alpha\beta}F^{\alpha\beta} - \frac{1}{4}\epsilon^{\alpha\beta\rho\sigma}(k_{AF})_{\alpha}A_{\beta}F_{\rho\sigma} + |D_{\mu}\phi|^2 + (k_{\phi\phi})^{\mu\nu}(D_{\mu}\phi)^*(D_{\nu}\phi) - U(|\phi|), \quad (1)$$

where  $A_{\mu}$  is the Abelian gauge field, and  $F_{\mu\nu} = \partial_{\mu}A_{\nu} - \partial_{\nu}A_{\mu}$  is the electromagnetic strength tensor. The four-vector  $(k_{AF})_{\alpha}$  is the CFJ background with mass dimension +1. The coupling between the gauge field and Higgs field  $\phi$  is given by the minimal covariant derivative  $D_{\mu}\phi = \partial_{\mu}\phi - ieA_{\mu}\phi$ , where  $e$  is the electric charge.

The LV in the Higgs sector is ruled by the CPT-even real symmetric and dimensionless tensor  $(k_{\phi\phi})^{\mu\nu}$ . The stationary Gauss law is

$$\partial_j \partial_j A_0 - (k_{AF})_i B_i = -e \mathcal{J}_0, \quad (2)$$

with  $\mathcal{J}_0 = [1 + (k_{\phi\phi})_{00}] J_0 - (k_{\phi\phi})_{0i} J_i$ , and  $J_\mu = i [\phi (D_\mu \phi)^* - \phi^* D_\mu \phi]$  is the conserved current density in absence of LV. Equation (2) shows clearly that the vectorial back-ground  $(k_{AF})_i$  is responsible for the coupling between electric and magnetic sectors, allowing the occurrence of electrically charged vortex solutions.

Similarly that happens in the MCSH model [15, 16], we must modify the model in (1) by introducing a neutral scalar field  $\Psi$  such that the new model supporting vortex solutions is

$$\begin{aligned} \mathcal{L} = & -\frac{1}{4} F_{\alpha\beta} F^{\alpha\beta} - \frac{1}{4} \epsilon^{\alpha\beta\rho\sigma} (k_{AF})_\alpha A_\beta F_{\rho\sigma} + |D_\mu \phi|^2 \\ & + (k_{\phi\phi})^{\mu\nu} (D_\mu \phi)^* (D_\nu \phi) + \frac{1}{2} \partial_\mu \Psi \partial^\mu \Psi \\ & - e^2 [1 + (k_{\phi\phi})_{00}] \Psi^2 |\phi|^2 - U(|\phi|, \Psi), \end{aligned} \quad (3)$$

and the potential  $U(|\phi|, \Psi)$  providing charged BPS vortices is

$$U = \frac{1}{2} [ev^2 - e\eta |\phi|^2 - (k_{AF})_3 \Psi]^2, \quad (4)$$

where  $\eta$  is defined in terms of the parity-even components of the Lorentz-violating Higgs tensor

$$\eta = \sqrt{[1 - (k_{\phi\phi})_{\theta\theta}] [1 - (k_{\phi\phi})_{rr}]}. \quad (5)$$

It can be observed that this potential provides two vacua states, one symmetric  $[\phi = 0, \Psi = ev^2 / (k_{AF})_3]$  and another asymmetric, responsible for generating topological BPS vortices  $[\Psi = 0, |\phi| = v/\eta^{1/2}]$ . The Higgs field vacuum expectation value gains contributions from Lorentz-violating terms introduced in Higgs sector.

### A. BPS formalism

We are interested to find self-dual equations or BPS [29] which are first-order differential equations whose solutions also solve the second-order Euler-Lagrange equations guaranteeing minimum energy configurations. To carry out the BPS procedure, we first calculate the stationary energy density of the model,

$$\begin{aligned} \mathcal{E} = & \frac{1}{2} B^2 + \frac{1}{2} [ev^2 - e\eta |\phi|^2 - (k_{AF})_3 \Psi]^2 \\ & + [\delta_{jk} - (k_{\phi\phi})_{jk}] (D_j \phi)^* (D_k \phi) + \frac{1}{2} (\partial_k A_0)^2 \\ & + \frac{1}{2} (\partial_k \Psi)^2 + e^2 [1 + (k_{\phi\phi})_{00}] [(A_0)^2 + \Psi^2] |\phi|^2, \end{aligned} \quad (6)$$

which is positive definite as long as the matrix  $\delta_{jk} - (k_{\phi\phi})_{jk}$  is positive definite and  $(k_{\phi\phi})_{00} > -1$ .

In a similar way as it is done in MCSH model [30, 31], the next step in the BPS procedure is to impose the condition  $\Psi = \mp A_0$ , in the energy density (6), which becomes

$$\begin{aligned} \mathcal{E} = & \frac{1}{2} B^2 + \frac{1}{2} [ev^2 - e\eta |\phi|^2 \pm (k_{AF})_3 A_0]^2 \\ & + [\delta_{jk} - (k_{\phi\phi})_{jk}] (D_j \phi)^* (D_k \phi) \\ & + (\partial_k A_0)^2 + 2e^2 [1 + (k_{\phi\phi})_{00}] (A_0)^2 |\phi|^2. \end{aligned} \quad (7)$$

We now introduce a modified vortex ansatz [20] which considers Lorentz-violating contributions

$$\begin{aligned} \phi &= \frac{v}{\sqrt{\eta}} g \exp\left(i\theta \frac{n}{\Lambda}\right), \\ A_\theta &= -\frac{1}{er} \left(a - \frac{n}{\Lambda}\right), \quad A_0 = \omega(r), \end{aligned} \quad (8)$$

where  $n$  is called the winding number, which expresses the topological character of fields. The parameter  $\Lambda$  depends only on the parity-even components of the matrix ruling LV in the Higgs sector:

$$\Lambda = \sqrt{\frac{1 - (k_{\phi\phi})_{\theta\theta}}{1 - (k_{\phi\phi})_{rr}}}. \quad (9)$$

The scalar functions  $g(r)$ ,  $a(r)$  and  $\omega(r)$  are regular, satisfying the boundary conditions

$$\begin{aligned} g(0) &= 0, \quad a(0) = \frac{n}{\Lambda}, \quad \omega'(0) = 0, \\ g(\infty) &= 1, \quad a(\infty) = 0, \quad \omega(\infty) = 0, \end{aligned} \quad (10)$$

these will be explicitly established below in Sec. II B.

Under (8), the Gauss law is now written as

$$\omega'' + \frac{\omega'}{r} - (k_{AF})_3 B = 2e^2 v^2 \Lambda \Delta \omega g^2, \quad (11)$$

where the magnetic field is  $B(r) = -\frac{a'}{er}$ , and the Lorentz-violating parameter  $\Delta$  is given by

$$\Delta = \frac{1 + (k_{\phi\phi})_{00}}{\Lambda \eta} > 0. \quad (12)$$

By replacing the ansatz (8) in (7) and by using Eq. (11) the energy density becomes written as a sum of square terms plus one term proportional to the magnetic field and a total divergence,

$$\begin{aligned} \mathcal{E} = & \frac{1}{2} \left( B \mp [ev^2 (1 - g^2) \pm (k_{AF})_3 \omega] \right)^2 \\ & + \frac{v^2}{\Lambda} \left( g' \mp \Lambda \frac{ag}{r} \right)^2 \pm ev^2 B \pm v^2 \frac{(ag^2)'}{r} + \frac{(r\omega\omega')'}{r}. \end{aligned} \quad (13)$$

The energy will be minimized by equating quadratic terms to zero, obtaining the self-dual equations

$$g' = \pm \Lambda \frac{ag}{r}, \quad (14)$$

$$B = -\frac{a'}{er} = \pm ev^2 (1 - g^2) + (k_{AF})_3 \omega, \quad (15)$$

both together Gauss's law in Eq. (11) describe electrically charged configurations which will be referred as CPT-odd vortices. The first of these equations, (14), has modifications due to LV present in the Higgs sector.

Under BPS equations, the energy density reads

$$\mathcal{E}_{BPS} = \pm ev^2 B \pm v^2 \frac{(ag^2)'}{r} + \frac{(r\omega\omega')'}{r}, \quad (16)$$

whose integration under boundary conditions (10) provides the total BPS energy

$$E_{BPS} = \pm ev^2 \int d^2 r B = \pm ev^2 \Phi = \pm 2\pi v^2 \frac{n}{\Lambda}, \quad (17)$$

which remains proportional to the magnetic flux, which, besides being proportional to the winding number, also depends explicitly on LV belonging to the Higgs sector.

We use BPS equations and Gauss's law to express energy density as a sum of positive terms:

$$\mathcal{E}_{BPS} = B^2 + 2\Lambda v^2 \left(\frac{ag}{r}\right)^2 + 2e^2 v^2 \Lambda \Delta (\omega g)^2 + (\omega')^2, \quad (18)$$

it is positive definite because  $\Lambda, \Delta > 0$ .

Also from Gauss's law in (11), the total charge of the self-dual vortices is

$$Q = 2\pi \int_0^\infty dr r q_0 = \frac{(k_{AF})_3 \Phi}{e} = 2\pi \frac{(k_{AF})_3}{e} \frac{n}{\Lambda}, \quad (19)$$

where  $q_0 = -2ev^2 \Lambda \Delta \omega g^2$ , is the electric charge density. The result is that the total electric charge is proportional to  $n/\Lambda$  just as the magnetic flux is.

### B. Asymptotic behavior

The asymptotic behavior is studied by solving BPS equations (14) and (15) together with Gauss's law (11) at the limits  $r \rightarrow 0$  and  $r \rightarrow \infty$ .

At the origin, the field profiles has the following behavior:

$$g(r) = Gr^n + \dots, \quad (20)$$

$$a(r) = \frac{n}{\Lambda} - \frac{1}{2}[ev^2 + (k_{AF})_3 \omega_0]er^2 + \dots, \quad (21)$$

$$\omega(r) = \omega_0 + \frac{1}{4}[ev^2 + (k_{AF})\omega_0](k_{AF})_3 r^2 + \dots, \quad (22)$$

where  $\omega_0 = \omega(0)$ . Equation (21) describes the behavior of  $a(r)$  close to origin, and it justifies the new ansatz

imposed in Eq. (8). On the other hand, Eq. (22) shows explicitly that the electric field at the origin must be null,  $\omega'(0) = 0$ .

It can be shown this model supports ANO vortex solutions whose characteristic behavior, at  $r \rightarrow \infty$ , for field profiles is

$$\begin{aligned} 1 - g(r) &\sim r^{-1/2} e^{-\beta r}, \\ a(r) &\sim r^{1/2} e^{-\beta r}, \\ \omega(r) &\sim r^{-1/2} e^{-\beta r}, \end{aligned} \quad (23)$$

where  $\beta$  is a real and positive parameter related to the spatial extension of the vortex, given by

$$\begin{aligned} \beta &= \frac{1}{2} \sqrt{[(k_{AF})_3]^2 + 2e^2 v^2 \Lambda (\sqrt{\Delta} + 1)^2} \\ &\quad - \frac{1}{2} \sqrt{[(k_{AF})_3]^2 + 2e^2 v^2 \Lambda (\sqrt{\Delta} - 1)^2}. \end{aligned} \quad (24)$$

This shows that for fixed  $(k_{AF})_3$ , the asymptotic behavior of the vortex profiles is ruled by the Lorentz-violating parameters belonging to the Higgs sector. Under such circumstance we have two interesting situations: The first one occurs when  $\Delta = 1$ ,  $\Lambda = 1$ , and  $\beta$  behaves as

$$\beta \rightarrow \frac{1}{2} \sqrt{[(k_{AF})_3]^2 + 8e^2 v^2} - \frac{1}{2} |(k_{AF})_3|. \quad (25)$$

Such a value is exactly the same ruling the asymptotic behavior of MCSH vortices. The second interesting case occurs when  $\Delta$  takes sufficiently large values ( $\Delta \gg (k_{AF})_3$ ):

$$\beta \rightarrow ev\Lambda^{1/2}\sqrt{2}, \quad (26)$$

This value corresponds to the usual MH model with Lorentz violation only in the Higgs sector, and it can be verified explicitly in Ref. [20]. On the other hand, by fixing the Lorentz-violating parameters of the Higgs sector and sufficiently large values of  $(k_{AF})_3$ ,  $\beta$  behaves as

$$\beta \rightarrow \frac{2e^2 v^2}{(k_{AF})_3} \Lambda \sqrt{\Delta}, \quad (27)$$

which is the mass scale of a CSH model with Lorentz-violating terms only in the Higgs sector.

### C. Numerical analysis

In order to perform numerical analysis, we use dimensionless coordinates and fields. We define the dimensionless coordinate  $\rho = ev\Lambda^{1/2}r$  and perform the following

field redefinitions:

$$g(r) \rightarrow g(\rho), \quad a(r) \rightarrow \frac{a(\rho)}{\Lambda}, \quad \omega(r) \rightarrow \frac{v}{\Lambda^{1/2}}\omega(\rho),$$

$$B(r) \rightarrow ev^2 B(\rho), \quad \mathcal{E}_{BPS}(r) \rightarrow \frac{v^2}{\Lambda} \mathcal{E}_{BPS}(\rho), \quad (28)$$

$$(k_{AF})_3 \rightarrow ev\Lambda^{1/2}\kappa.$$

With these new definitions, we rewrite the BPS equations and Gauss's law:

$$g' = \pm \frac{ag}{\rho}, \quad (29)$$

$$-\frac{a'}{\rho} = \pm (1 - g^2) + \kappa\omega, \quad (30)$$

$$\omega'' + \frac{\omega'}{\rho} + \kappa \frac{a'}{\rho} = 2\Delta\omega g^2. \quad (31)$$

It can be observed that if  $\Delta = 1$ , Eqs. (29-31) looks exactly like the ones in MCSH model. The set of equations will be solved by using the following boundary condition:

$$g(0) = 0, \quad a(0) = n, \quad \omega'(0) = 0, \quad (32)$$

$$g(\infty) = 1, \quad a(\infty) = 0, \quad \omega(\infty) = 0. \quad (33)$$

Also the BPS energy density is expressed by

$$\mathcal{E}_{BPS}(\rho) = B^2 + 2 \left( \frac{ag}{\rho} \right)^2 + 2\Delta(\omega g)^2 + (\omega')^2; \quad (34)$$

it will be positive definite whenever  $\Delta > 0$ .

The dimensionless  $\beta$  mass scale reads

$$\beta = \frac{1}{2} \sqrt{\kappa^2 + 2 \left( \sqrt{\Delta} + 1 \right)^2} - \frac{1}{2} \sqrt{\kappa^2 + 2 \left( \sqrt{\Delta} - 1 \right)^2}. \quad (35)$$

Below, we depict the profiles obtained from numerical solutions of Eqs. (29-31) under boundary conditions (33) for  $\kappa = 1$ ,  $n = 1$  and some values for  $\Delta$ . Because the BPS energy density (34) is positive definite for  $\Delta > 0$ , we consider two regions  $0 < \Delta < 1$  (green lines) and  $\Delta > 1$  (red lines), in which the behavior of solutions are different. There are two interesting values of  $\Delta$  which allow to obtain two well-know models: The first one is  $\Delta = 1$  (solid black lines) whose profiles correspond to MCSH model, and the second value is the limit  $\Delta \rightarrow \infty$ , when MH model (solid blue lines) is attained.

Figures 1 and 2 depict the profiles of the Higgs and vector fields, respectively. It is observed that they reach the asymptotic values rapidly for  $\Delta > 1$  and saturate more slowly for  $\Delta < 1$ , as is expected from Eq. (35) for fixed  $\kappa$ . Also, it is verified explicitly that the solutions for  $1 < \Delta < \infty$  (red lines) are confined between the MCSH (solid black line) and MH (solid blue line) models.

Such that the profiles are narrower when  $\Delta > 1$ , and the maximum narrowing is attained when  $\Delta \rightarrow \infty$  (solid blue line) where the MH model is recovered. On the other hand, for  $0 < \Delta < 1$ , the profiles get more spread out, occupying a larger area when  $\Delta \rightarrow 0$ . In this limit, the vector potential has a very light decay, by which we can infer that the magnetic field corresponding to this values will have low intensity.

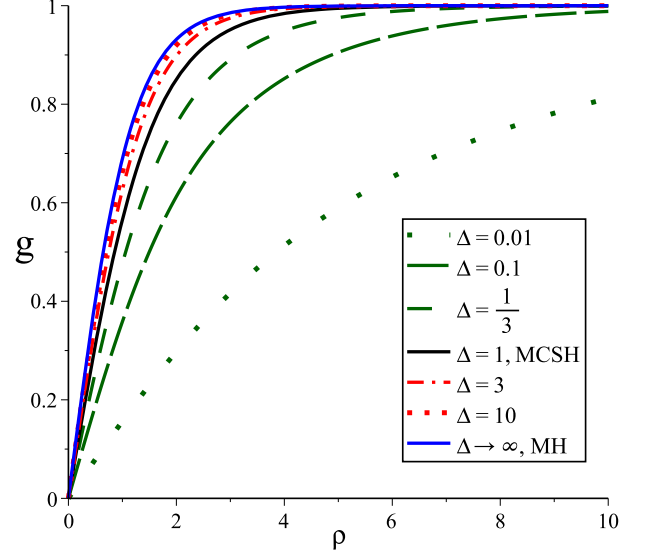


FIG. 1: Scalar field  $g(\rho)$ .

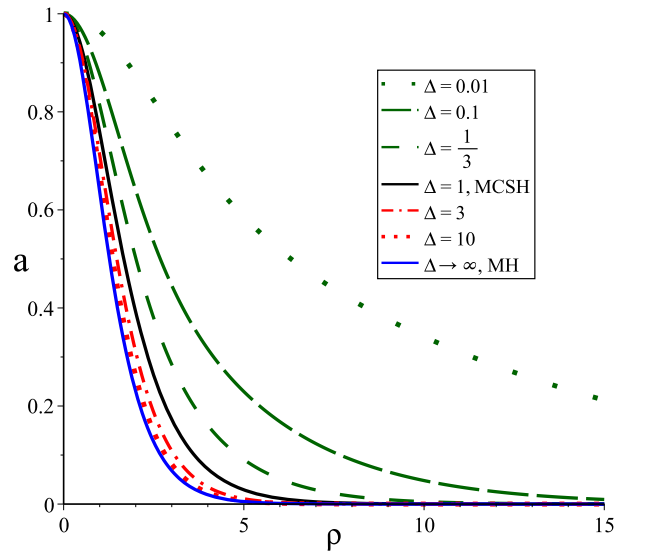


FIG. 2: Vector potential  $a(\rho)$ .

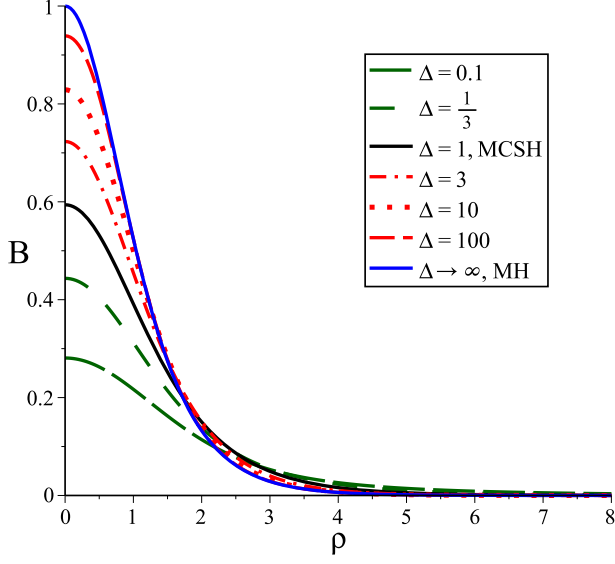
FIG. 3: Magnetic field  $B(\rho)$ .

Figure 3 shows the profiles for the magnetic field which are lumps centered at the origin. For increasing values of  $\Delta$ , the profiles are narrower and have higher amplitude in such a way the maximum narrowing and maximum intensity are reached when  $\Delta \rightarrow \infty$  (solid blue line). For  $0 < \Delta < 1$ , the profiles have less intensity and are more spread when  $\Delta \rightarrow 0$ . Higher amplitudes are obtained for the values  $1 < \Delta < \infty$ ; such profiles are located between the MCSH ( $\Delta = 1$ , solid black line) and the MH profile ( $\Delta \rightarrow \infty$ , solid blue line). At infinity, the magnetic field vanishes more rapidly as  $\Delta$  increases.

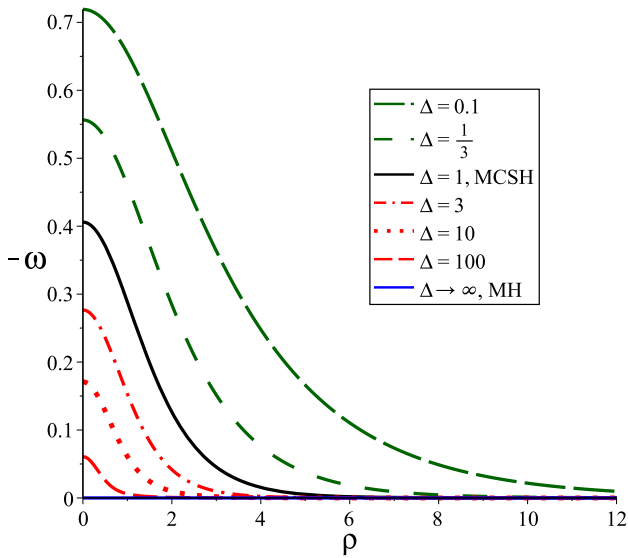
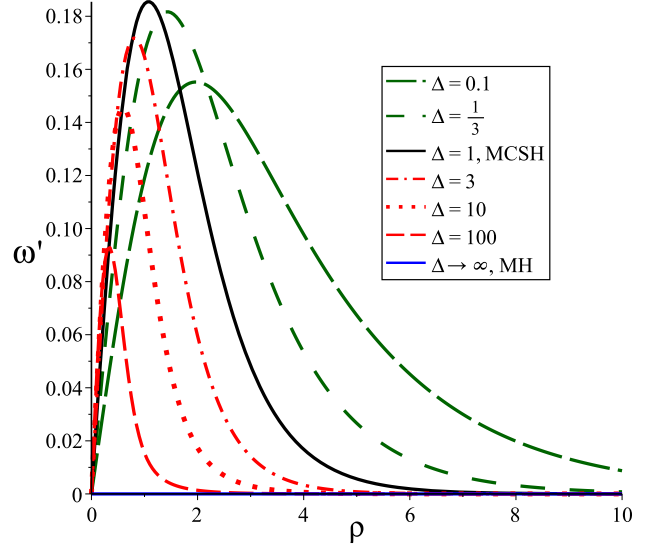
FIG. 4: Scalar potential  $\omega(\rho)$ .FIG. 5: Electric field  $\omega'(\rho)$ .

Figure 4 depicts the profiles for the scalar potential. For  $\Delta > 1$ , the CFJ parameter is less relevant for increasing values of  $\Delta$ , such that the profiles become smaller, and in the limit  $\Delta \rightarrow \infty$  (solid blue line), the profile overlaps the horizontal axis, implying that vortices become electrically uncharged such as in the MH model. On the other hand, in the interval  $0 < \Delta < 1$ , the scalar potential profiles are more extended and with greater intensity at the origin. For this range of  $\Delta$ , the CFJ parameter becomes more relevant when  $\Delta \rightarrow 0$ .

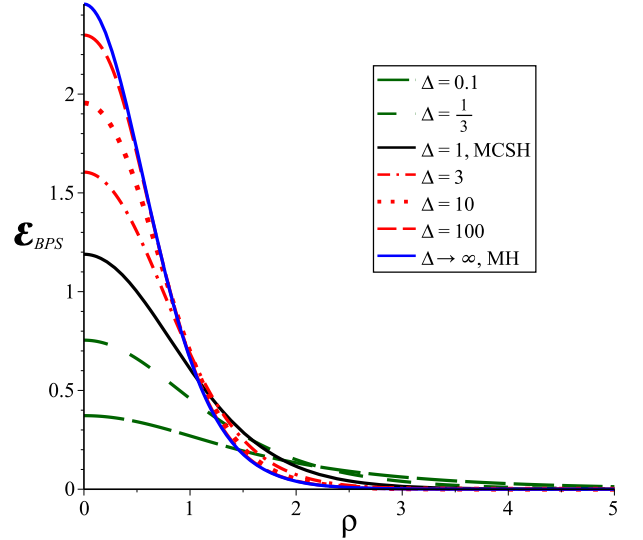
FIG. 6: Energy density  $\mathcal{E}_{BPS}(\rho)$ .

Figure 5 describes the behavior for the electric field. For  $n = 1$ , the maximum electric field intensity is reached for  $\Delta = 1$  (solid black line), corresponding to MCSH model. The electric field gets radially spread out for de-



creasing values of  $\Delta$ . On the other hand, for  $\Delta > 1$ , the electric field is located closer to the origin and decays rapidly for increasing values of  $\Delta$ . In the limit  $\Delta \rightarrow \infty$ , the electric field disappears, which result agrees with electrically uncharged vortex models.

Figure 6 describes BPS energy density profiles, which for  $n = 1$  are lumps centered at origin. For increasing values of  $\Delta$ , we have higher amplitudes at the origin which sharply decay, reaching zero rapidly, which corresponds to well-located vortices. On the other hand, when  $\Delta \rightarrow 0$ , amplitude decreases at the origin and reaches zero slowly, implying a more extended, large energy density distribution but with little intensity. The profiles of BPS energy density have the same behavior as the magnetic field profiles.

### III. TOPOLOGICAL CHARGED BPS VORTICES IN A CPT-EVEN AND LORENTZ-VIOLATING FRAMEWORK

In this section, we investigate the formation of topological electrically charged BPS vortices in a Lorentz-violating MH model, where both the gauge and Higgs sector contain CPT-even and Lorentz-violating terms [2]. Specifically, we analyze the nonbirefringent Lorentz violating coefficients of the electromagnetic sector of SME. This model is a natural generalization of earlier studies performed in Refs.[20, 21]. The Lagrangian density for this model describing charged vortices is

$$\mathcal{L} = -\frac{1}{4}F_{\mu\nu}F^{\mu\nu} - \frac{1}{2}\kappa^{\rho\alpha}F_{\rho\sigma}F_{\alpha}^{\sigma} + |D_{\mu}\phi|^2 + (k_{\phi\phi})^{\mu\nu}(D_{\mu}\phi)^*(D_{\nu}\phi) - U(|\phi|) . \quad (36)$$

In stationary regime, Gauss's and Ampere's law are

$$L_{ij}\partial_i\partial_j A_0 + \epsilon_{ija}\kappa_{0i}\partial_j B_a = -e\mathcal{J}_0 , \quad (37)$$

$$M_{jbc}\partial_b B_c - \kappa_{0i}\partial_j\partial_i A_0 + \kappa_{0j}\partial_j\partial_i A_0 = e\mathcal{J}_i , \quad (38)$$

respectively. The matrix  $L_{ij} = (1 + \kappa_{00})\delta_{ij} - \kappa_{ij}$  is symmetric and positive definite which carries parity-even and CPT-even Lorentz-violating coefficients. The density  $\mathcal{J}_0$  is the same defined after Eq. (2). In Ampere's law, we have defined the tensor  $M_{jbc} = \epsilon_{jbc} - \epsilon_{jac}\kappa_{ab} - \kappa_{ja}\epsilon_{abc}$ , and current density  $\mathcal{J}_i = J_i - (k_{\phi\phi})_{ij}J_j + (k_{\phi\phi})_{0i}J_0$ , with  $J_{\mu}$  also defined after Eq. (2). We observe that parity-odd coefficients  $\kappa_{0i}$  and  $(k_{\phi\phi})_{0i}$  are responsible for electric and magnetic sector coupling however some  $(k_{\phi\phi})_{0i}$  do not contribute to the formation of vortex solutions.

As was shown in Ref. [21], the model (36) must be

modified to supports BPS solutions:

$$\begin{aligned} \mathcal{L} = & -\frac{1}{4}F_{\mu\nu}F^{\mu\nu} - \frac{1}{2}\kappa^{\rho\alpha}F_{\rho\sigma}F_{\alpha}^{\sigma} \\ & + |D_{\mu}\phi|^2 + (k_{\phi\phi})^{\mu\nu}(D_{\mu}\phi)^*(D_{\nu}\phi) \\ & + \frac{1}{2}(1 + \kappa_{00})\partial_{\mu}\Psi\partial^{\mu}\Psi + \frac{1}{2}\kappa^{\mu\nu}\partial_{\mu}\Psi\partial_{\nu}\Psi \\ & - e^2[1 + (k_{\phi\phi})_{00}]\Psi^2|\phi|^2 - U(|\phi|, \Psi) . \end{aligned} \quad (39)$$

The interaction term  $U(|\phi|, \Psi)$  given by

$$U(|\phi|, \Psi) = \frac{(ev^2 - e\eta|\phi|^2 - \epsilon_{ij}\kappa_{0i}\partial_j\Psi)^2}{2(1-s)} \quad (40)$$

contains a derivative coupling and a  $|\phi|^4$ -potential, which provides BPS configurations. Above we have define the parameter  $s = \kappa_{11} + \kappa_{22} = \kappa_{rr} + \kappa_{\theta\theta}$ .

#### A. BPS formalism

In order to implement the BPS formalism, we first write down the stationary energy density

$$\begin{aligned} \mathcal{E} = & \frac{1}{2}L_{ij}(\partial_i A_0)(\partial_j A_0) + \frac{1}{2}(1-s)B^2 \\ & + [\delta_{ij} - (k_{\phi\phi})_{ij}](D_i\phi)^*(D_j\phi) + \frac{1}{2}L_{ij}\partial_i\Psi\partial_j\Psi \\ & + e^2[1 + (k_{\phi\phi})_{00}][(A_0)^2 + \Psi^2]|\phi|^2 + U(|\phi|, \Psi) . \end{aligned} \quad (41)$$

It is positive-definite whenever  $s < 1$ ,  $(k_{\phi\phi})_{00} > -1$ , and  $\delta_{ij} - (k_{\phi\phi})_{ij}$ , a positive-definite matrix.

By following a similar procedure to that used in the previous model, we impose condition  $\Psi = \mp A_0$ , in the energy density (41), which becomes

$$\begin{aligned} \mathcal{E} = & \frac{1}{2}(1-s)B^2 + \frac{(ev^2 - e\eta|\phi|^2 \pm \epsilon_{ij}\kappa_{0i}\partial_j A_0)^2}{2(1-s)} \\ & + [\delta_{ij} - (k_{\phi\phi})_{ij}](D_i\phi)^*(D_j\phi) \\ & + L_{ij}(\partial_i A_0)(\partial_j A_0) + 2e^2[1 + (k_{\phi\phi})_{00}](A_0)^2|\phi|^2 . \end{aligned} \quad (42)$$

Now we introduce the vortex ansatz (8) to express Gauss's law as follows:

$$(1 + \lambda_r)\left(\omega'' + \frac{\omega'}{r}\right) - \kappa_{0\theta}\frac{(rB)'}{r} = 2e^2v^2\Lambda\Delta\omega g^2, \quad (43)$$

with  $\lambda_r = \kappa_{00} - \kappa_{rr}$ . Afterwards rewriting the energy density (42) by using the ansatz (8), we use Eq. (43) to

express it in the following convenient form:

$$\begin{aligned} \mathcal{E} = & \frac{1}{2}(1-s) \left[ B \mp \frac{ev^2(1-g^2) \mp \kappa_{0\theta}\omega'}{1-s} \right]^2 \\ & + \frac{v^2}{\Lambda} \left[ g' \mp \Lambda \frac{ag}{r} \right]^2 \pm ev^2 B \pm v^2 \frac{(ag^2)'}{r} \\ & + (1+\lambda_r) \frac{(r\omega\omega')'}{r} - \kappa_{0\theta} \frac{(r\omega B)'}{r}. \end{aligned} \quad (44)$$

It is minimized by equating quadratic terms to zero, providing self-dual or BPS equations

$$g' = \pm \Lambda \frac{ag}{r}, \quad (45)$$

$$B = -\frac{a'}{er} = \pm \frac{ev^2(1-g^2)}{1-s} - \frac{\kappa_{0\theta}\omega'}{1-s}, \quad (46)$$

both together with Gauss's law in Eq. (43) describe electrically neutral configurations, which will be called as CPT-even vortices. The total electric charge of the topological vortices is zero, as can explicitly shown by integrating Gauss's law in Eq. (43) under boundary conditions given in Eqs. (55) and (56):

$$Q = 4\pi ev^2 \Lambda \Delta \int_0^\infty dr r \omega g^2 = 0. \quad (47)$$

Whenever the BPS equations are satisfy, the BPS energy density is

$$\begin{aligned} \mathcal{E}_{BPS} = & \pm ev^2 B \pm v^2 \frac{(ag^2)'}{r} \\ & + (1+\lambda_r) \frac{(r\omega\omega')'}{r} - \kappa_{0\theta} \frac{(r\omega B)'}{r}, \end{aligned} \quad (48)$$

whose integration under boundary conditions established in Eqs. (55) and (56) provides total BPS energy

$$E_{BPS} = \pm ev^2 \int B d^2x = \pm 2\pi v^2 \frac{n}{\Lambda}, \quad (49)$$

where the magnetic flux, such as in the previous model, besides being proportional to the winding number, also depends explicitly on LV belonging to the Higgs sector.

We use BPS equations and Gauss's law to express energy density as

$$\begin{aligned} \mathcal{E}_{BPS} = & (1-s) B^2 + 2\Lambda v^2 \left( \frac{ag}{r} \right)^2 \\ & + 2e^2 v^2 \Lambda \Delta (g\omega)^2 + (1+\lambda_r) (\omega')^2; \end{aligned} \quad (50)$$

it is positive-definite for  $s < 1$  and  $\lambda_r > -1$ .

## B. Boundary conditions

By solving BPS equations (45 and 46) and Gauss's law (43) at  $r = 0$ , we obtain

$$g(r) = G_n r^n + \dots, \quad (51)$$

$$a(r) = \frac{n}{\Lambda} - \frac{e^2 v^2 (1+\lambda_r)}{2\Sigma} r^2 + \dots, \quad (52)$$

$$\omega(r) = \omega_0 + \frac{ev^2 \kappa_{0\theta}}{\Sigma} r + \dots, \quad (53)$$

where  $\omega_0 = \omega(0)$  and

$$\Sigma = (\kappa_{0\theta})^2 + (1-s)(1+\lambda_r). \quad (54)$$

Therefore, the boundary conditions at the origin are

$$g(0) = 0, \quad a(0) = \frac{n}{\Lambda}, \quad \omega'(0) = \frac{ev^2 \kappa_{0\theta}}{\Sigma} \quad (55)$$

The model also supports ANO vortices, whose behavior when  $r \rightarrow \infty$  is given by Eq. (23), so the boundary conditions for the field profiles at infinity are

$$g(\infty) = 1, \quad a(\infty) = 0, \quad \omega(\infty) = 0, \quad (56)$$

but now the mass scale  $\beta$  is

$$\beta = ev\Lambda^{1/2} \sqrt{\frac{\beta_1 \pm \beta_2}{\Sigma}}, \quad (57)$$

where

$$\beta_1 = (1+\lambda_r) + \Delta(1-s), \quad (58)$$

$$\beta_2 = \sqrt{[(1+\lambda_r) - \Delta(1-s)]^2 - 4\Delta(\kappa_{0\theta})^2}, \quad (59)$$

and  $\beta_1, \beta_2$  are positive real numbers. For  $\beta_2$ , the condition  $4\Delta(\kappa_{0\theta})^2 \leq [(1+\lambda_r) - \Delta(1-s)]^2$  must be satisfied. The signals will be used as follows:  $+$  ( $-$ ) for  $(1+\lambda_r) - \Delta(1-s) > 0$  ( $< 0$ ).

When  $\kappa_{0\theta} = 0$ , the Eq. (57) recovers the mass scale of electrically uncharged BPS vortices,

$$\beta = ev\Lambda^{1/2} \sqrt{\frac{2}{1-s}}, \quad (60)$$

already obtained in Ref. [20].

On the other hand, when  $\beta_2 = 0$ , the parity-odd coefficient can be expressed in terms of parity-even ones,

$$\kappa_{0\theta} = \pm \frac{|1+\lambda_r - \Delta(1-s)|}{2\sqrt{\Delta}}, \quad (61)$$

and the mass scale becomes

$$\beta = ev\Lambda^{1/2} \sqrt{\frac{4\Delta}{(1+\lambda_r) + \Delta(1-s)}}. \quad (62)$$

Another interesting possibility is to set  $s = 0$  and  $\lambda_r = 0$  in Eq.(57); i.e., we can consider null parity-even electromagnetic coefficients, getting

$$\beta = ev\Lambda^{1/2} \sqrt{\frac{1 + \Delta \pm \sqrt{(1 - \Delta)^2 - 4\Delta(\kappa_{0\theta})^2}}{1 + (\kappa_{0\theta})^2}}, \quad (63)$$

with signal  $+$  ( $-$ ) for  $1 - \Delta > 0$  ( $< 0$ ), respectively. This situation also provides ANO-like vortices whenever

$$(1 - \Delta)^2 \geq 4\Delta(\kappa_{0\theta})^2 \quad (64)$$

is satisfied. We remark that in the absence of LV in Higgs sector ( $\Delta = 1$ ) (see Ref. [21]), it is impossible to obtain ANO vortices when  $s$  and  $\lambda_r$  are nulls, because the mass scale (63) becomes a complex number.

### C. Numerical analysis

Under the same coordinate rescaling and field redefinitions as in (28) but with  $\kappa_{0\theta} \rightarrow \kappa$ , the dimensionless BPS equations and Gauss's law are

$$g' = \pm \frac{ag}{\rho}, \quad (65)$$

$$-\frac{a}{\rho} = \pm \frac{(1 - g^2)}{(1 - s)} - \frac{\kappa}{(1 - s)}\omega', \quad (66)$$

$$(1 + \lambda_r) \left( \omega'' + \frac{\omega'}{\rho} \right) - \kappa \frac{(\rho B)'}{\rho} = 2\Delta g^2 \omega. \quad (67)$$

We can see that for  $\kappa \rightarrow -\kappa$ , the solutions change as  $g \rightarrow g$ ,  $a \rightarrow a$ ,  $\omega \rightarrow -\omega$ .

On the other hand, the BPS energy density is given by

$$\begin{aligned} \mathcal{E}_{BPS}(\rho) &= (1 - s)B^2 + 2 \left( \frac{ag}{\rho} \right)^2 \\ &\quad + 2\Delta(g\omega)^2 + (1 + \lambda_r)(\omega')^2, \end{aligned} \quad (68)$$

is defined positive providing that  $s < 1$ ,  $\Delta > 0$ ,  $\lambda_r > -1$ .

#### 1. A charged vortex configuration

Now we consider the following configuration to solve numerically the dimensionless Eqs. (65)-(67):

$$\lambda_r = 0, \quad s = 0, \quad \kappa = \frac{\Delta - 1}{2\sqrt{\Delta}}, \quad \Delta > 0. \quad (69)$$

In this case, the boundary conditions are expressed as

$$\begin{aligned} g(0) &= 0, \quad a(0) = n, \quad \omega'(0) = \frac{2(\Delta - 1)\sqrt{\Delta}}{(1 + \Delta)^2}, \\ g(\infty) &= 1, \quad a(\infty) = 0, \quad \omega(\infty) = 0. \end{aligned} \quad (70)$$

The mass scale  $\beta$  is given by

$$\beta = 2\sqrt{\frac{\Delta}{(1 + \Delta)}}, \quad (71)$$

and we note that for  $\Delta \ll 1$ , the defect reaches its asymptotic values slowly. But when  $\Delta \sim 1$ , the behavior is close to the MH profiles (see below, Figs. 7–12, solid black lines), because  $\beta \rightarrow \sqrt{2}$ , MH mass scale. On the other hand, for  $\Delta \rightarrow \infty$ , the mass scale reaches its maximum value  $\beta \rightarrow 2$  (see below, Figs. 7-9,11,12, solid blue lines).

Below, we depict the profiles obtained from numerical solutions of the Eqs. (65)-(67) under boundary conditions (70). Without loss of generality, we set  $n = 1$ . Because the BPS energy density is positive definite for  $\Delta > 0$ , we consider two regions  $0 < \Delta < 1$  (green lines) and  $\Delta > 1$  (red lines) in which the behavior of solutions are different. The solutions are always compared with profiles of MH model (solid black lines).

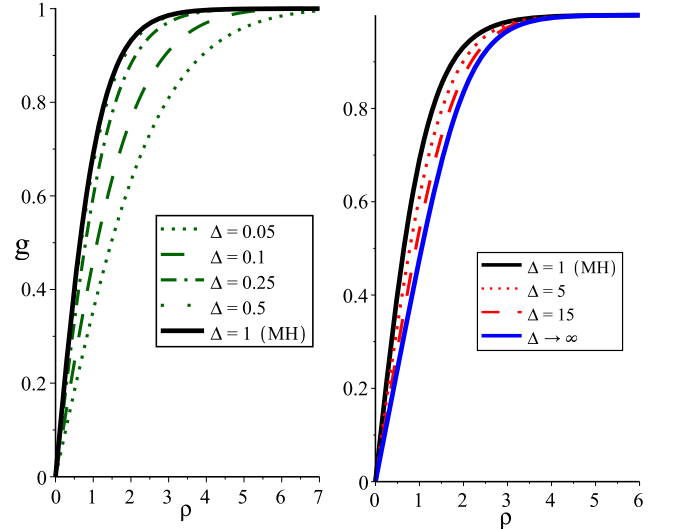


FIG. 7: Higgs field  $g(\rho)$ . Left-side represents the profiles for  $0 \leq \Delta \leq 1$  and right-side for  $\Delta \geq 1$ .

Figure 7 shows the profiles of the Higgs field. For  $\Delta \ll 1$ , they are very spread and reach their asymptotic value slowly. But when  $\Delta \rightarrow 1$ , they are narrower and attain the vacuum state more rapidly. For  $0 \leq \Delta \leq 1$ , the profiles are limited by the usual MH solution  $\Delta = 1$  (solid black line). For  $\Delta > 1$ , the profiles are wider than the MH one, but such increment is limited by the profile obtained when  $\Delta \rightarrow \infty$  (solid blue line).



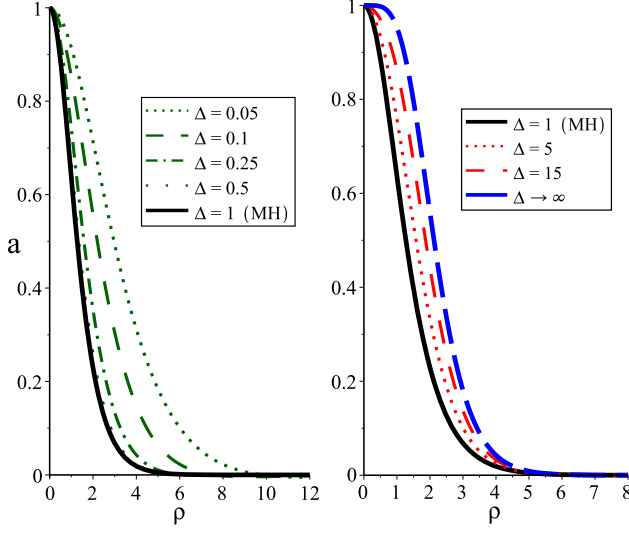
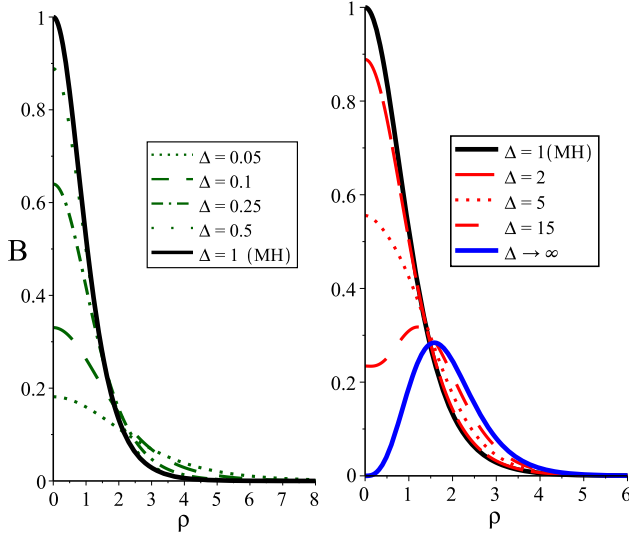
FIG. 8: Vector potential  $a(\rho)$ .

Figure 8 depicts the profiles of the vector potential. For  $0 < \Delta < 1$ , the profiles are wider when  $\Delta \rightarrow 0$ , and narrower when  $\Delta \rightarrow 1$ . The maximum narrowing is attained in  $\Delta = 1$ , where MH model (solid black line) is recover. For  $\Delta > 1$ , the profiles becomes wider when  $\Delta$  increases, but the incremented width has a limit that is attained when  $\Delta \rightarrow \infty$  (solid blue line).

FIG. 9: Magnetic field  $B(\rho)$ .

The magnetic field profiles are shown in Fig. 9, whose amplitudes at origin are given by  $4\Delta/(\Delta+1)^2$ . For the range  $0 < \Delta \leq 1$  (green lines), they are lumps centered at origin with increasing amplitudes whenever  $\Delta$  increases, whose maximum value is reached for  $\Delta = 1$  (MH model). For  $\Delta > 1$ , the amplitude decreases when  $\Delta$  increases continuously. An interesting fact is observed

around  $\Delta \sim 6$ : the lump format of the magnetic field begins to deform, transforming in a ringlike profile. In the limit  $\Delta \rightarrow \infty$ , it has a null value at the origin such that the ring profiles resemble those of CSH and MCSH models.

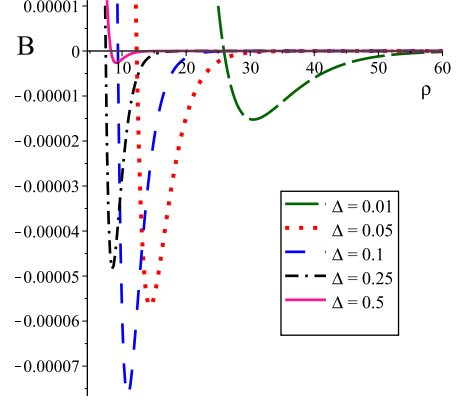


FIG. 10: Magnetic flux inversion.

The model has localized magnetic flux inversion when  $0 \leq \Delta < 1$ , such as it is shown in Fig. 10, where a zoom was performed for the profiles with  $0.01 \leq \Delta \leq 0.5$ . One can clearly observe the localized magnetic flux inversion, which is more pronounced for values  $\Delta < 0.5$ . For  $\Delta > 0.5$ , such inversion does not exist. This peculiarity in this Lorentz-violating MH model was also observed in the absence of LV in Higgs sector [21]. Thus, we can say that such localized magnetic flux inversion is a proper effect of CPT-even and Lorentz-violating terms.

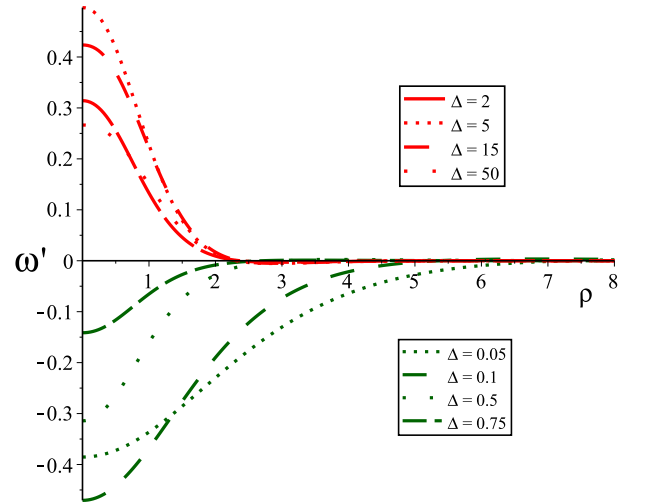
FIG. 11: Electric field  $\omega'(\rho)$ .

Figure 11 shows the electric field profiles, which are lumps centered at origin, whose amplitudes are given by Eq. (70). It is negative for  $0 < \Delta < 1$ , taking its minimum value  $-1/2$ , when  $\Delta = 3 - 2\sqrt{2} \sim 0.172$ , and it is

positive for  $\Delta > 1$ , taking its maximum value  $1/2$ , when  $\Delta = 3 + 2\sqrt{2} \sim 5.828$ . The electric field is null when  $\Delta \rightarrow 0, 1, \infty$ .

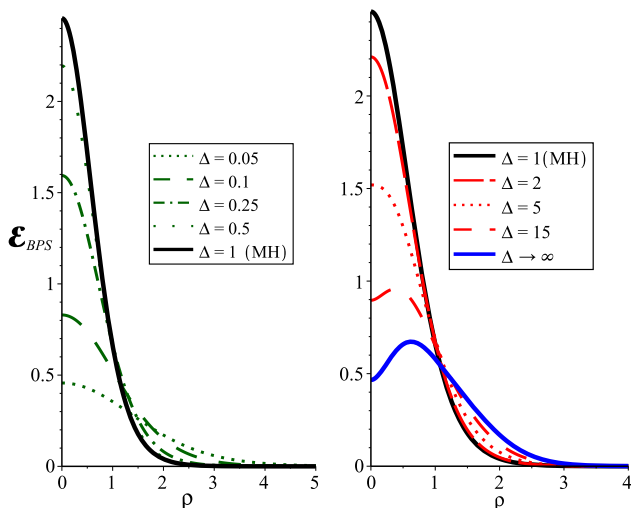


FIG. 12: BPS energy density  $\mathcal{E}(\rho)$ .

Figure 12 presents the profiles for the BPS energy density, which are similar to magnetic field ones due to the direct relation between energy and magnetic flux. For  $0 < \Delta < 1$ , they are lumps centered at the origin whose amplitude increases when  $\Delta$  increases, attaining its maximum value in  $\Delta = 1$ , which reproduces the BPS energy density of the MH model. For  $\Delta > 1$ , the lumps decrease in their amplitudes, but around  $\Delta \sim 6$ , they transform in rings. Such ring-like behavior is maintained for all values of  $\Delta > 6$ , and their amplitudes at origin decrease whenever  $\Delta$  increases continuously such that in the limit  $\Delta \rightarrow \infty$ , the amplitude is  $\sim 0.46$  (but for  $n > 1$ , the amplitude at origin is zero). The ringlike behavior resembling the CSH and MCSH behaviors is an interesting effect of LV in the Higgs sector.

#### IV. REMARKS AND CONCLUSIONS

We have performed a comprehensive analysis on the formation of charged BPS vortices in the context of the SME. Two cases were studied separately. First, we have discussed the Abelian MH model supplemented with the CFJ term in electromagnetic sector and a CPT-even Lorentz-violating term in the Higgs sector. The second case analyzed is also the Abelian MH model but this time provided with CPT-even and Lorentz-violating terms in both the photon and Higgs sectors. We have verified that for supporting charged BPS vortex solutions the original models must be modified by introducing a neutral scalar field  $\Psi$ , with appropriate dynamic. This procedure is similar to the one that happens in MCSH model. Notwithstanding, there are some differences between the CPT-odd and CPT-even charged vortices: In

the CPT-odd case, both the charge density and the total charge are non-null whereas, in the CPT-even case, the charge density is nonzero, but the total electric charge is null. Another important result involves the magnetic flux, which, besides being proportional to the winding number, also depends explicitly in the Lorentz-violating coefficients belonging to the Higgs sector, such as presented in Eqs. (17) and (49). This result was firstly obtained in the context of uncharged BPS vortices in SME [20], and it appears to be a general effect produced by the CPT-even and Lorentz-violating terms of the Higgs sector.

One of the observations already made in Ref.[20] is the change of the vortex ansatz (8) describing the profiles of the Higgs and gauge fields. This is an important fact because the boundary condition satisfied by gauge field at origin [see Eqs. (55) and (10)] is modified by LV belonging to Higgs sector. Otherwise, the solutions of self-dual or BPS equations will not be topological; neither will have finite energy. Such change in gauge field boundary conditions are crucial for the new characteristic presented by the quantized magnetic flux.

Our analysis shows that for fixed LV in photon sector, the LV in Higgs sector increases the richness of BPS solutions in the context of SME. For example, the presence of LV in Higgs sector allows to interpolate CPT-odd vortices between very spread for  $0 < \Delta < 1$ , to some more localized ones when  $\Delta \rightarrow 1$ . For  $1 \leq \Delta < \infty$ , profiles run from the MCSH ( $\Delta = 1$ ) to the MH ( $\Delta \rightarrow \infty$ ) solutions. For the CPT-even vortices, the profiles in the region  $0 < \Delta \leq 1$ , are wider and more spread for decreasing  $\Delta$ . But now the value  $\Delta = 1$ , represents the vortex solution of MH model. For  $\Delta > 1$  and increasing  $\Delta$ , the vortex profiles are confined between the MH model (solid black line) and the one obtained when ( $\Delta \rightarrow \infty$ ) (solid blue line). An interesting fact in CPT-even vortices is the appearance of ringlike profiles (for magnetic field and BPS energy density) for sufficiently large values of  $\Delta$  parameter, as explicitly shown in Figs. 9 and 12, respectively. Another peculiarity is the localized magnetic flux inversion, such as was also observed in the absence of LV in Higgs sector [21]. This property appears to be a typical effect of CPT-even and Lorentz-violating terms in photon sector.

A remark on the subject of considering large values for Lorentz-violation coefficients: In the context of standard model extension, the Lorentz-violating parameters must be sufficiently small. However, as energy positivity is preserved whenever  $\Delta > 0$ , we can consider large values of  $\Delta$  within an effective model describing the electrodynamics of some type of material media.

In this context we, can also comment about implication of these Lorentz-violating models in superconductivity physics. The new materials presenting high-temperature superconductivity are anisotropic; most of them have a layered structure. The simplest GL model is for an uniaxial superconductor whose free energy density is written

as

$$\mathcal{F} = \frac{B^2}{8\pi} + \alpha |\phi|^2 + \frac{\beta}{2} |\phi|^2 + \gamma_{jk} \left( i\hbar \partial_j \phi^* - \frac{2e}{c} A_j \phi^* \right) \left( -i\hbar \partial_k \phi - \frac{2e}{c} A_k \phi \right), \quad (72)$$

where  $B$  is the magnetic field produced by the gauge field  $A_k$  and  $\beta$  is a constant, but  $\alpha$  depends in temperature changing its sign at  $T = T_c$ , and  $\gamma_{jk}$  is a constant tensor coupled to the crystal axes.

It is possible to establish a connection between the Lorentz-violating models whose energy densities are given by Eqs. (7), (42) and the free energy (72) describing a high- $T_c$  superconductor. Such connection is provided by the term  $[\delta_{ij} - (k_{\phi\phi})_{ij}] (D_i \phi)^* (D_j \phi)$ , which allows to relate the matrix  $\delta_{ij} - (k_{\phi\phi})_{ij}$ , with the tensor  $\gamma_{jk}$ . It is clear that in both LV models, the coefficients do not depend in temperature as happens in phenomenolog-

ical Ginzburg-Landau's models. The study of possible contributions to superconductivity can be obtained by analyzing the nonrelativistic limits of both LV models at finite temperature. Such approach would allow to analyze Lorentz-violations effects or contributions in London free energy, the Josephson effect, the interaction of vortices with the crystalline structure (the vortex's intrinsic pinning), and resistivity, among others. Advances in such interesting research would be developed in a future manuscript.

Future developments can be oriented to analyze the influence of Lorentz violation in the existence of topological defects in the non-Abelian sector of the standard model—i.e., magnetic monopoles and non-Abelian vortices in the context of standard model extension. The results will be reported soon.

### ACKNOWLEDGMENTS

The authors thank CAPES, CNPq and FAPEMA (Brazilian agencies) for financial support.

- 
- [1] D. Colladay and V. A. Kostelecky, Phys. Rev. D **55**, 6760 (1997).
  - [2] D. Colladay and V. A. Kostelecky, Phys. Rev. D **58**, 116002 (1998).
  - [3] S. R. Coleman and S. L. Glashow, Phys. Rev. D **59**, 116008 (1999).
  - [4] S.M. Carroll, G.B. Field and R. Jackiw, Phys. Rev. D **41**, 1231 (1990).
  - [5] V. A. Kostelecky and M. Mewes, Phys. Rev. Lett. **87**, 251304 (2001).
  - [6] V. A. Kostelecky and M. Mewes, Phys. Rev. D **66**, 056005 (2002); V. A. Kostelecky and M. Mewes, Phys. Rev. Lett. **97**, 140401 (2006).
  - [7] B. Altschul, Nucl. Phys. B **796**, 262 (2008); B. Altschul, Phys. Rev. Lett. **98**, 041603 (2007); C. Kaufhold and F. R. Klinkhamer, Phys. Rev. D **76**, 025024 (2007).
  - [8] F.R. Klinkhamer and M. Risse, Phys. Rev. D **77**, 016002 (2008); **77**, 117901 (2008).
  - [9] F. R. Klinkhamer and M. Schreck, Phys. Rev. D **78**, 085026 (2008).
  - [10] A. A. Abrikosov, Zh. Eksp. Teor. Fiz. **32**, 1442 (1957), [Sov. Phys. JETP **5**, 1174 (1957)].
  - [11] V. L. Ginzburg and L. D. Landau, Zh. Eksp. Teor. Fiz. **20**, 1064 (1950); This paper was published in English in the volume: L. D. Landau, Collected Papers (Pergamon Press, Oxford, 1965), p. 546.
  - [12] H. Nielsen, P. Olesen, Nucl. Phys. **B 61**, 45 (1973).
  - [13] S. Deser, R. Jackiw, and S. Templeton, Ann. Phys. (NY) **140**, 372 (1982); Gerald V. Dunne, arXiv:hep-th/9902115.
  - [14] R. Jackiw and E. J. Weinberg, Phys. Rev. Lett. **64**, 2234 (1990); R. Jackiw, K. Lee, and E.J. Weinberg, Phys. Rev. D **42**, 3488 (1990); J. Hong, Y. Kim, and P.Y. Pac, Phys. Rev. Lett. **64**, 2230 (1990); G.V. Dunne, Self-Dual Chern-Simons Theories (Springer, Heidelberg, 1995).
  - [15] C.k. Lee, K.M. Lee, H. Min, Phys. Lett. B **252**, 79 (1990).
  - [16] S. Bolognesi and S.B. Gudnason, Nucl. Phys. B **805**, 104 (2008).
  - [17] M.N. Barreto, D. Bazeia, R. Menezes, Phys.Rev.D **73**, 065015 (2006); A. de Souza Dutra, M. Hott, and F. A. Barone, Phys. Rev. D **74**, 085030 (2006); D. Bazeia, M. M. Ferreira Jr., A. R. Gomes, R. Menezes, Physica D **239**, 947 (2010); A. de Souza Dutra, R. A. C. Correa, Phys. Rev. D **83**, 105007 (2011).
  - [18] N.M. Barraz Jr., J.M. Fonseca, W.A. Moura-Melo, J.A. Helayël-Neto, Phys.Rev. D **76**, 027701 (2007); A. P. Baêta Scarpelli and J. A. Helayël-Neto, Phys.Rev. D **73**, 105020 (2006).
  - [19] M.D. Seifert, Phys. Rev. Lett. **105**, 201601 (2010); Phys. Rev. D **82**, 125015 (2010).
  - [20] C. Miller, R. Casana, M. M. Ferreira, Jr., and E. da Hora, Phys.Rev. D **86**, 065011 (2012).
  - [21] R. Casana, M. Ferreira, Jr., E. da Hora, and C. Miller, Phys. Lett. B **718**, 620 (2012).
  - [22] R.Casana, L. Sourrouille, Phys. Lett. B **726**, 488 (2013).
  - [23] R. Casana, M. M. Ferreira, E. Da Hora, A. B. F. Neves, arXiv:1309.4247 [hep-th].
  - [24] L. Sourrouille, Phys. Rev. D **89**, 087702 (2014).
  - [25] Z. Hao and C. R. Hu, Phys. Rev. B **48**, 16818 (1993); J. Low Temp. Phys. **104**, 265 (1996).
  - [26] D. L. Feder and C. Kallin Phys. Rev. B **55**, 559 (1996).
  - [27] J. R. Clem, Z. Hao, L. Dobrosavljevic-Grujic, Z. Radovic, Jour. Low Temp. Phys. **88**, 213 (2001).
  - [28] N. Kopnin, *Vortices in type-II superconductors: structure and dynamics, Part II – Anisotropic and layered superconductors* (Orsay, 1996).
  - [29] E. B. Bogomol'nyi, Sov. J. Nuc. Phys. **24**, 449 (1976); M. Prasad and C. Sommerfield, Phys. Rev. Lett. **35**, 760 (1975).
  - [30] P.K. Ghosh, Phys. Rev. D **49**, 5458 (1994); T. Lee and H. Min, Phys. Rev. D **50**, 7738 (1994).
  - [31] N. Sakai and D. Tong, J. High Energy Phys. **03** (2005) 019; G. S. Lozano, D. Marques, E. F. Moreno, and F. A. Schaposnik, Phys. Lett. B **654**, 27 (2007).